Desalination and Water Treatment
www.deswater.com

doi: 10.5004/dwt.2017.21661

97 (2017) 79–86
November

Effects of membrane and operational features on biofouling in a pressure retarded osmosis process

Taek-Seung Kim[a], Pengfei Sun[a], Yong-Gyun Park[b], Hee-Deung Park[a,*]

[a]*School of Civil, Environmental and Architectural Engineering, Korea University, Seoul 02841, Korea, Tel. +82-2-3290-4861; Fax: +82-2-928-7656; email: heedeung@korea.ac.kr (H.-D. Park)*
[b]*Environmental Process Engineering Team, GS Engineering & Construction, Seoul 03159, Korea*

Received 27 August 2017; Accepted 28 October 2017

ABSTRACT

Pressure retarded osmosis (PRO) is a technology that generates power via mixing two solutions having different salinity across a semipermeable membrane. Similar to other membrane-based technologies, PRO processes are prone to membrane biofouling. In this study, the effects of membrane and operational features on the membrane biofouling of a PRO process were investigated, through a comparison with those of a reverse osmosis process. Surface roughness, charge, and hydrophobicity affected the propensity of the biofilm formation on the support layer of the PRO membrane. Nevertheless, these physical and chemical properties could not sufficiently explain the rapid flux decline of the PRO unit under an enhanced biofouling condition. Water flow from the feed solution to the draw solution, and the structural property of the PRO membrane resulted in the accumulation of microorganisms in the support matrix of the PRO membrane, which contributed significantly to the flux decline propensity. The results suggested that the pretreatment of feed solution and/or new membrane fabrication are needed to minimize the access of microorganisms in the support matrix for reducing membrane biofouling in PRO.

Keywords: Biofilm; Biofouling; Pressure retarded osmosis; Reverse osmosis; Support matrix

1. Introduction

Pressure retarded osmosis (PRO) is a technology in which renewable energy is obtained from the osmotic pressure formed between a high salinity draw solution and a low salinity feed solution across a semipermeable membrane [1–3]. Osmosis enables water to pass through the semipermeable membrane from the feed solution to the draw solution, which dilutes the draw solution and increases its volume. Pressure is then added to the diluted draw solution, and a portion of the diluted draw solution is depressurized by a hydroturbine to generate power [4,5]. Similar to other membrane-based technologies, PRO processes are vulnerable to membrane fouling [6–8]. Membrane fouling reduces water flux across the membrane [6–8] and increases pressure drop in the feed solution side and/or the draw solution side [6], which decreases power production and increases the energy cost of operating the PRO processes. The PRO processes are thus less viable as net energy producing processes.

Membrane fouling can be classified into organic fouling, inorganic fouling, colloidal/particulate fouling, and biofouling, depending on the nature of the foulants [9,10]. Organic, inorganic, and colloidal/particulate fouling can be prevented to some extent by removing foulants in the feed water [11,12], while fouling formed on membrane surfaces can be removed by physical or chemical cleaning [7,8,13–16]. Microorganism-associated biofouling is relatively difficult to remove [6,11,17]. Although feed water pretreatments (e.g., biocide addition and filtration) can remove 99.99% of microorganisms, the residual microbial cells enter the membrane vessels and grow by attaching to the membrane surfaces [11]. Attached microorganisms on membrane surfaces are not easy

* Corresponding author.

to clean by physical or chemical methods [6,10,11], mostly due to the formation of biofilms, which are communities of microorganisms encapsulated by self-produced extracellular polymeric substances mostly consisting of carbohydrates, polysaccharides, and proteins [18–20].

Membrane biofouling in the PRO processes has been rarely studied compared with that in the reverse osmosis (RO) or forward osmosis process, which is a technology that uses a semipermeable membrane, similar to the PRO process. Until now, Bar-Zeev et al.'s [6] work is the only systematic study of membrane biofouling in a PRO process. They observed severe biofouling in the support layer of a PRO membrane and feed spacers, which resulted in ~50% water flux decline and ~250% pressure drop increase in a laboratory-scale PRO unit under an enhanced biofouling condition. Unlike the fouling associated with organics and inorganics [7], the biofouling could not be sufficiently removed by pressure-aided osmotic backwash (only 12% recovery of permeate water flux) due to the formation of irreversible fouling [6,17]. Based on this observation and the osmotic backwash test, they claimed that the PRO process would not be viable without the proper treatment of biofouling.

Although Bar-Zeev et al. [6] introduced biofouling development and its impact on the PRO performance (e.g., water flux), the way in which a biofouling event is affected by the physical and chemical properties of a PRO membrane and the operational characteristics of PRO (e.g., passage of water across a membrane from the feed solution side to the draw solution side) have not been studied. Understanding of the biofouling in association with membrane and operational features is important because the study can provide insight into membrane synthesis and process operation for biofouling reduction and, ultimately, the operation of a viable PRO process in terms of net energy production.

The aim of this study was to correlate the membrane and operational features with biofouling in a PRO process. First, we analyzed the physical (e.g., surface morphology, membrane structure, and roughness) and chemical properties (e.g., surface charge and hydrophobicity) of a model PRO membrane. Second, to study the effect of the physical and chemical features of a PRO membrane on biofouling, biofilms were formed on the membrane using a model bacterium under a flow condition without pressure. Third, to investigate the effect of the operational features of a PRO process on membrane biofouling, a laboratory-scale PRO unit was operated under an enhanced biofouling condition. With the purpose of determining the unique features of membrane biofouling in the PRO process, all of the experiments were conducted by comparing the membrane biofouling in the RO process.

2. Materials and methods

2.1. Bacterium and membrane

Pseudomonas aeruginosa was used as a model bacterium that causes biofouling in PRO and RO processes. This bacterium is often detected in osmosis processes such as RO process [19,21,22]. *P. aeruginosa* was cultured in tryptic soy broth (TSB; BD, Franklin Lakes, NJ, USA) at 250 rpm and 37°C using a shaking incubator. CSM-PRO-3 membrane (Toray Chemical Korea, Seoul, Korea) and SWC5 membrane (Hydranautics Nitto Denko, Oceanside, CA, USA) were used for the model PRO and RO membrane, respectively.

2.2. Scanning electron microscopy

Surface and cross-sectional images of the PRO and RO membranes were acquired using a field emission-scanning electron microscope (SU-70, Hitachi, Tokyo, Japan). Dried membrane coupons were coated using a platinum ion-sputter coater (E-1030, Hitachi, Tokyo, Japan) for 90 s. Magnifications were ×700, ×20,000, and ×500 for the cross-sectional, active, and support layers of the virgin membranes, respectively, at a voltage of 15 kV. For the observation of biofouled membranes, a pretreatment process was conducted before observation. The biofouled membranes were initially immersed in 4% glutaraldehyde solution for 1 h at 4°C. Afterward, the cross-sectional, active, and support layer membranes were sequentially immersed in 50%, 80%, and 100% ethyl alcohol for 15 min, respectively, for dehydration. The dehydrated membranes were dried in a desiccator overnight. Magnifications were ×5,000, ×3,000, and ×3,000 for the cross-sectional, active, and surface layers of the biofouled membranes, respectively, at a voltage of 15 kV.

2.3. Atomic force microscope analysis

An atomic force microscopy (AFM; PUCOStation; Surface Imaging Systems, Herzogenrath, Germany) was used to evaluate the surface roughness of the membranes. The average surface roughness (S_a) and root mean square roughness (R_{RMS}) were analyzed for the active layer of the RO membrane and support layer of the PRO membrane, respectively. Analytical conditions were 0.4–0.6 N/m approaching force, 0.7 line/s scanning speed, and 10 μm × 10 μm scan area. Scanned images of the surface layer were used to calculate S_a and R_{RMS} values using the SPIP software (Surface Imaging Systems).

2.4. Contact angle measurement

The hydrophobicity of the membranes and the model bacterium was evaluated by measuring the contact angle. For the measurement of membrane hydrophobicity, membrane coupons were prepared (5.5 cm length × 2.5 cm width) and attached to glass slides using double-sided tape. For the measurement of bacterial hydrophobicity, a biomass layer was prepared by filtering a bacterial solution through a 0.1 μm polyvinylidene fluoride membrane (Durapore membrane filter, Millipore, Billerica, MA, USA). The bacterial solution was prepared by collecting the bacterial cells (OD at 595 nm = 1.0) at a speed of ×8,000*g* for 10 min using a centrifuge and then resuspending the collected cells in 10 mL deionized (DI) water by pipetting two times. The membrane coupons and the biomass layer were dried in a desiccator before measurement. The Phoenix 300 static contact angle analyzer (Surface Electro Optics, Suwon, South Korea) based on the pendent drop principle was used to measure the contact angles by dropping 10 μL DI water on the membrane surfaces or biomass layer.

2.5. Zeta potential analysis

Zeta potential analysis was used to measure the surface charges of the membranes and the model bacterium.

The monitoring solution was prepared from 10 mL NaCl solution (0.01 M) with 20 μL monitor solution containing polyamide micelles (Otsuka Electronics, Osaka, Japan). The zeta potential of the membranes was evaluated by laser Doppler method [23] in a solid sample cell unit using an analyzer (ELSZ-1000, Photal, Otsuka Electronics). The zeta potential of the model bacterium in 0.01 M NaCl solution was measured in a flow cell device using the same analyzer as that used for measuring the zeta potential of the membrane surfaces.

2.6. Biofilm formation test

Biofilm formation on the membranes was evaluated using a drip-flow biofilm reactor (DFR 110, BioSurface Technologies, Bozeman, MT, USA). Initially, the membrane coupons (2.5 cm width × 5 cm length) were inserted into the channels of the DFR. To develop biofilms on the coupons, a bacterial solution was dripped onto the biofilm reactor at 0.3 mL/min for 24 h. The bacterial solution was prepared by adding 10 mL *P. aeruginosa* culture (OD at 595 nm = 1.0) in 1 L TSB. After cessation of the biofilm reactor operation, the membrane coupons were washed twice with 1 mL of sterilized phosphate-buffered saline (137 mM NaCl, 2.7 mM KCl, 10 mM Na_2HPO_4, 2 mM KH_2PO_4; pH = 7.2). The coupons were then treated with 4′,6-diamidino-2-phenylindole (DAPI; Carl Roth, Karlsruhe, Germany) solution for 15 min in a dark room. Unbound DAPI was washed twice using 1 mL DI water. The biofilms were observed using a confocal laser scanning microscopy (CLSM; Carl Zeiss LSM700, Jena, Germany). Biofilms were captured using a *z*-stack mode of the CLSM for acquisition of three-dimensional (3-D) images. The CLSM images were obtained using a ×20 objective lens (Plan-APOCHROMAT 20×/0.8, Carl Zeiss). The biofilm images were used to assess the biovolume ($\mu m^3/\mu m^2$) and thickness (μm) of the biofilms formed on the membrane coupons using the ImageJ software (National Institutes of Health, Bethesda, MD, USA).

2.7. Operation of PRO and RO units

Laboratory-scale PRO and RO units (Fig. 1) were operated to compare the performances of the two processes under an enhanced biofouling condition. The dimensions of the PRO membrane cell were 7.7 cm length, 2.6 cm height, and 0.3 cm channel height, while those of the RO membrane cell were 5 cm length, 5 cm height, and 0.3 cm channel height. Before and after the operation of the PRO and RO units, cleaning was conducted to remove residual organic foulants and bacteria based on a previous study [18] as follows: (1) circulation of 0.5% NaOCl solution for 2 h, (2) rinsing the units three times for 10 min using tap water, (3) cleaning the units using 0.6 g/L sodium dodecyl sulfate at pH 11 for 30 min, (4) repetition of step 2, (5) sterilization of the units using 98% ethanol for 1 h, (6) repetition of step 2, and (7) rinsing the units three times using DI water for elimination of residual ethanol. The volume of each cleaning solution in the PRO unit was 3 L for the feed solution loop and 6 L for the draw solution loop, while that in the RO unit for feed solution was 6 L.

Synthetic wastewater was used as a feed solution of the PRO unit and RO unit, while synthetic seawater RO brine was used for a draw solution of the PRO unit. Synthetic wastewater [18] was composed of 1.16 mM sodium citrate, 0.94 mM NH_4Cl, 0.45 mM KH_2PO_4, 0.5 mM $CaCl_2{\cdot}2H_2O$, 0.5 mM $NaHCO_3$, 2.0 mM NaCl, 0.6 mM $MgSO_4{\cdot}7H_2O$, and 0.02% d-glucose. Synthetic seawater RO brine [7] was composed of 56.2 mM Na_2SO_4, 123.0 mM $MgCl_2$, 3.78 mM $NaHCO_3$, 23.2 mM $CaCl_2$, and 831.62 mM NaCl.

In order to achieve a stable permeate flux, the PRO unit was prerun for 2 h using DI water for both the draw and the feed solution loop. The operation was conducted at 10 bar and 0.4 L/min for the draw solution loop, and at 0.4 bar and 0.4 L/min for the feed solution loop. Afterward, the PRO unit was operated at the same condition for 24 h using 6 L synthetic seawater RO brine for the draw solution loop and using 3 L synthetic wastewater with and without 50 mL bacterial solution (OD at 595 nm = 0.1) for the feed solution loop. Similar to the PRO unit, the RO unit was preoperated at 25 bar and 0.9 L/min for 15 h using DI water. Afterward, the RO unit was run at the same condition for 24 h using 4 L synthetic wastewater amended with and without 62.5 mL bacterial solution (OD at 595 nm = 0.1) as the feed water.

3. Results

3.1. Physical characteristics of the PRO and RO membranes

For the analysis of the morphology of the PRO and RO membranes, scanning electron microscopic (SEM) images of the cross-section, active, and support layers was

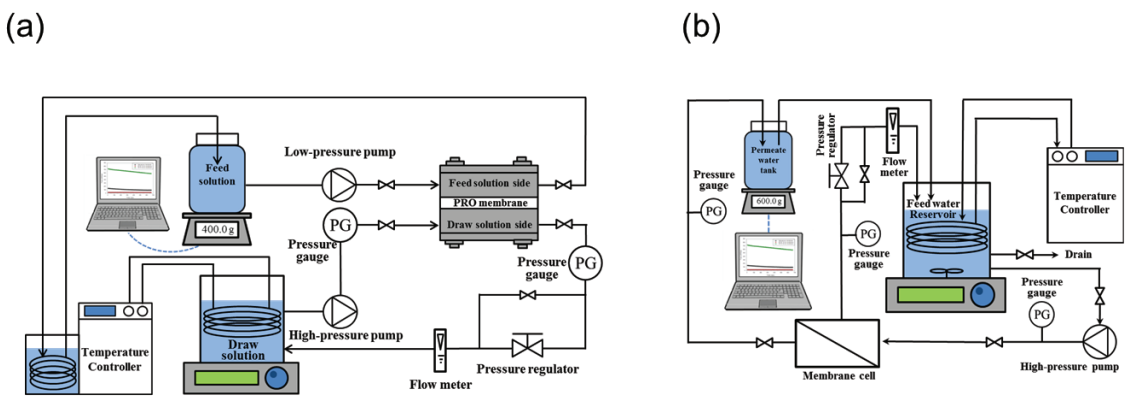

Fig. 1. Schematic diagram of the laboratory-scale PRO (a) and RO (b) units.

obtained (Fig. 2). The cross-sectional images demonstrated that the two membranes were asymmetric structures consisting of dense active and loose support layers. The active layers of the PRO and RO membranes had similar morphologies (i.e., peak and valley structures [22]). However, the support layers of the two membranes had different morphologies. The lattice pattern of the textile under the smooth polysulfone layer was visible in the PRO membrane. It is also noted that crevices were observed near the crossing points between the weft and warp threads (see arrows in Fig. 2). In the case of the RO membrane, non-woven fabric was exposed without a layer.

For the analysis of the surface roughness of the PRO and RO membranes, S_a and R_{RMS} roughness was evaluated using an AFM analyzer. The roughness of the support layer was evaluated for the PRO membrane because feed water containing microorganisms crosses the PRO membrane from the support layer in the PRO processes [6]. On the other hand, the roughness of the active layer was evaluated for the RO membrane because feed water containing microorganisms crosses the RO membrane from the active layer in the RO processes [18,24]. As shown in Fig. 3, the active layer of the RO membrane was ~1.9 times rougher than the support layer of the PRO membrane, as evaluated from the S_a and R_{RMS} roughness.

3.2. Chemical characteristics of the PRO and RO membranes

Zeta potential was analyzed to evaluate the surface charge of the membranes and the model bacterium as a function of pH from 5 to 9. Similar to the roughness analysis, the support layer of the PRO membrane and the active layer of the RO membrane were evaluated. As shown in Fig. 4, both the PRO and the RO membranes showed negative zeta potentials in all pH conditions, although the RO membrane had slightly lower values (from –1.3 to –19.2 mV for the PRO membrane and from –6.2 to –26.7 mV for the RO membrane). On the other hand, the zeta potential tended to decrease with increasing pH. The model bacterium also showed negative zeta potentials in all pH conditions (from –45.9 to –52.9 mV), but the negative zeta potentials were greater than those of the membranes.

The contact angle of the membranes and the model bacterium was analyzed to evaluate their hydrophobicity. As shown in Fig. 5, the average contact angles were 60.6°, 74.8°, and 27.9° for the PRO membrane, the RO membrane, and the model bacterium, respectively. This result indicates that the model bacterium was less hydrophobic than the membranes, and the RO membrane was slightly more hydrophobic than the PRO membrane.

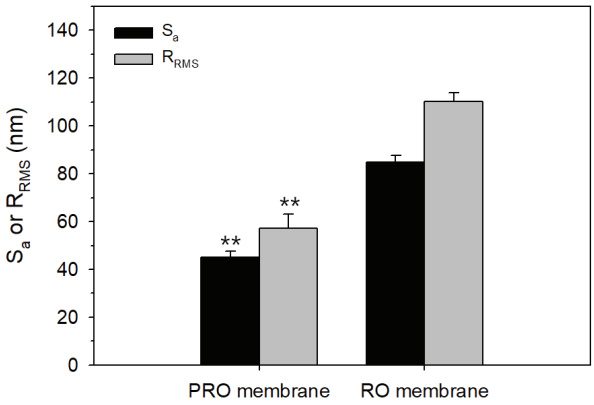

Fig. 3. Average surface roughness (S_a) and root mean square roughness (R_{RMS}) of support layer of the PRO membrane and active layer of the RO membrane analyzed by AFM. Error bars indicate standard deviations of three measurements. $^{**}P < 0.005$ vs. roughness of the RO membrane.

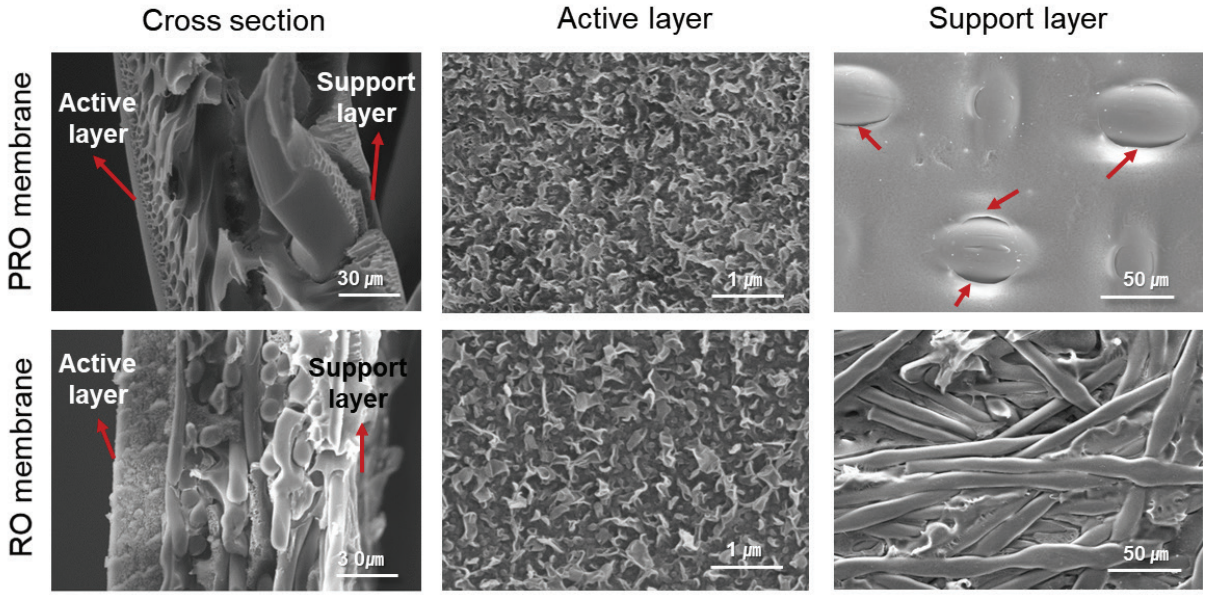

Fig. 2. SEM images of cross-section, active, and support layers of the PRO (upper row) and RO membranes (lower row) used in this study. Arrows indicate crevices observed on support layer of the PRO membrane.

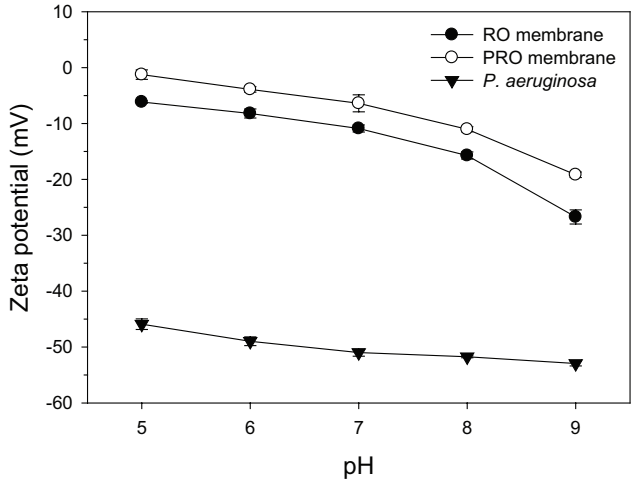

Fig. 4. Zeta potentials of support layer of the PRO membrane, active layer of the RO membrane, and a layer of *P. aeruginosa* cells ranging from pH 5 to 9. Error bars indicate standard deviations of three measurements.

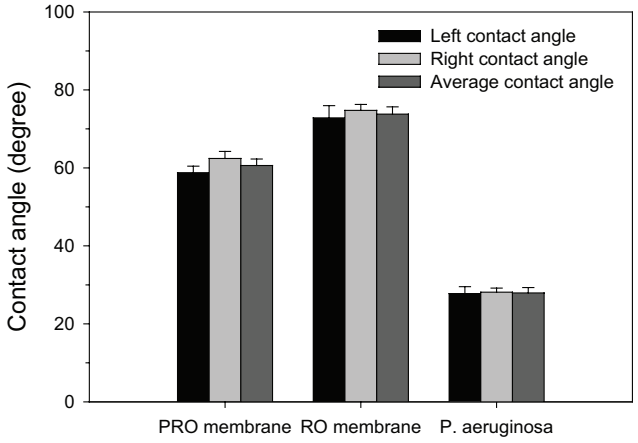

Fig. 5. Static contact angles of support layer of the PRO membrane, active layer of the RO membrane, and a layer of *P. aeruginosa* cells. Error bars indicate standard deviations of three measurements.

3.3. Biofilm formation on the PRO and RO membranes

Biofilms of the model bacterium were formed on the support layer of the PRO membrane and on the active layer of the RO membrane, using a DFR. The reactor was operated by dripping a bacterial solution onto the membranes. 3-D images of the biofilms grown on the membranes for 24 h were acquired using CLSM (Fig. 6(a)). Biofilms formed on the RO membrane were flat and dense, while those formed on the PRO membrane were relative rough and loose. Particularly, biofilms were rarely formed on the bumps of the PRO membrane. An analysis based on the CLSM images obtained by *z*-stack mode was performed to evaluate the average thickness and biovolume of the biofilms (Fig. 6(b)). The analysis demonstrated that the biofilms on the RO membrane were 34% thicker than those on the PRO membrane. In addition, the biofilms on the RO membrane had 40% larger biovolume than those on the PRO membrane.

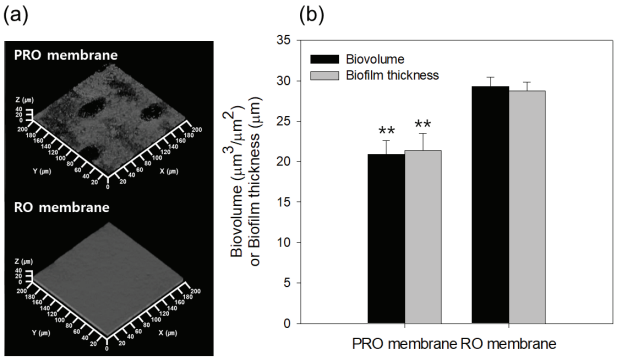

Fig. 6. Biofilms formed on support layer of the PRO membrane and active layer of the RO membrane. (a) CLSM images of 24-h biofilms. (b) Biofilm thickness and biovolume analyzed by the ImageJ software. Error bars indicate standard deviations of three measurements. $^{**}P < 0.01$ vs. thickness or biovolume of the biofilms formed on the RO membrane.

3.4. Process performance under an enhanced biofouling condition

Under an enhanced biofouling condition, changes in process performance were investigated using laboratory-scale PRO and RO units. After a prerun using DI water for 2 h, bacterial solution was added to the feed solution loop in order to increase the speed of the biofouling process on the membranes. The process performance was analyzed by measuring normalized water flux (J/J_0) as a function of operational time (Fig. 7). In the PRO unit with the addition of the bacterial solution, the normalized water flux declined from the beginning of the unit operation and reached 0.11 when the operational time ended (24 h). A significant decrease in the normalized water flux was also observed in the PRO unit without the addition of bacterial solution (J/J_0 = 0.72 at 24 h), which might be due to the dilution of the draw solution by the permeate water in the PRO unit operated via a closed loop (Fig. 1). Compared with the decline of the normalized water flux in the PRO unit, with the addition of the bacterial solution, the flux decline in the RO unit was not substantial up to 10 h of operation. Afterward, a significant flux decline was observed and the normalized water flux reached 0.20 when the operational time ended (24 h). Unlike the PRO unit, changes in the flux were not substantial (J/J_0 = 0.91 at 24 h) when the bacterial solution was not added. The results of comparing the process performance under an enhanced biofouling condition demonstrated that the PRO unit was more vulnerable to the addition of bacterial solution than the RO unit at the beginning of the operation.

4. Discussion

Microorganisms tend to adhere to solid surfaces and to form biofilms. Bacterial biofilms develop through initial bacterial attachment to a surface, microcolony formation, maturation into differentiated biofilm, and dispersal into planktonic cells [25]. Initial bacterial attachment is a critical step among the developmental stages [26], and begins by the mass transport of cells to a surface sufficiently close to lead to reversible attachment [27,28]. Palmer et al. [29] reported that reversible attachment is governed by van der Waals forces, electrostatic

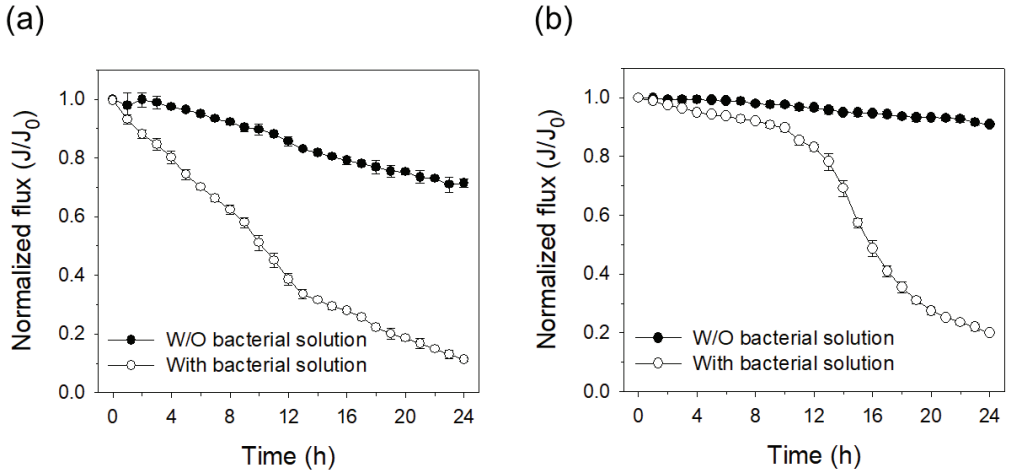

Fig. 7. Normalized flux (J/J_0) as a function of operational time monitored in the PRO unit (a) and the RO unit (b) operated with and without bacterial solution. Error bars indicate standard deviations of three measurements.

forces, and hydrophobic interactions, and is affected by diverse surface features such as roughness, surface charge, and hydrophobicity. Rougher surfaces are generally better for the attachment of bacterial cells due to the greater surface area for cell attachment [30,31]. Positively charged surfaces tend to pull bacterial cells because bacterial cells typically show negative charge at neutral pH. Hydrophobic surfaces are better for attaching bacterial cells than hydrophilic surfaces [32,33], although the reason is under debate [34,35].

In this study, fewer biofilms were formed on the PRO membrane than on the RO membrane (Fig. 6). Considering that the PRO membrane has a lower roughness and hydrophobicity than the RO membrane, the result of biofilm formation was expected. However, the opposite result would be expected if the surface charge factor was more influential in the initial bacterial attachment and subsequent biofilm formation than the roughness and hydrophobicity. Note that the RO membrane had more negative charge than the PRO membrane (Fig. 4). It appears that the combination of roughness and hydrophobicity was more important than the surface charge in our study. Because bacterial attachment on a surface involves a complex array of chemical and physical interactions [29], it is difficult to predict relative biofilm formation propensity based on limited information about membrane features.

Although the PRO membrane was less vulnerable to biofilm formation than the RO membrane (Fig. 6), flux decline in a PRO unit was more responsive to an enhanced biofouling condition from the beginning of unit operation than that in a RO unit (Fig. 7). This result suggests that the biofilm formation on the membrane surface was not the sole contributor of the flux decline in the PRO unit. As reported in the study by Bar-Zeev et al. [6], microorganisms can accumulate and form biofilm under the support layer (i.e., in the support matrix) in our study. This speculation was verified by observing cross-sectional images of the PRO membrane after cessation of the PRO unit operation using SEM (Fig. 8). A significant accumulation of bacterial cells was observed in the support matrix of the PRO membrane (see the arrows in the cross-sectional SEM image in Fig. 8). It is likely that microorganisms entered the support matrix through the crevices near the crossing points between the weft and warp threads of the support layer (Fig. 2) and accumulated there. It appears that the accumulation of bacterial cells in the support matrix was more influential than the biofilm formation on the support layer on the flux decline of the PRO unit. In the case of the top SEM images, similar to the results of biofilm formation (Fig. 6), fewer microorganisms were attached to the support layer of the PRO membrane than to the active layer of the RO membrane.

In order to block the accumulation of microbial cells in the support matrix, the support layer of the PRO membrane should not pass through the microorganisms. In the case of the model PRO membrane used in this study, the PRO membrane needs to be fabricated without crevices on the surface of the support layer (e.g., fabrication of a sealed support layer). However, this would decrease the water flux across the PRO membrane by decreasing the water permeability coefficient [8] and by increasing the membrane structural parameter [17]. Because the power density generated in PRO is the product of water flux and applied hydraulic pressure [8], the reduced water permeability coefficient and increased membrane structural parameter would decrease in power density. In other words, the fabrication of the PRO membrane that can block the entrance of microorganisms to the support matrix can prevent biofouling in the support matrix, but this would potentially reduce the power density in the PRO membrane. In the future, experiments will be necessary to evaluate the degree to which the blockage affects the power density.

The results associated with the biofilm formation (Fig. 6) and the flux decline (Fig. 7) suggest that biofouling development in the PRO membrane somewhat differed to that in the RO membrane. Fig. 9 shows the proposed conceptual model of the biofouling development between the two membranes. In the PRO membrane, the microorganisms move to the support layer of the membrane via water flow, attach onto the support layer, and form biofilms. Meanwhile, some of the cells pass through the support layer, accumulate in the support matrix, and form biofilms. This would result in rapid flux decline from the beginning. Similar to the biofilm formation in the PRO membrane, microorganisms move to

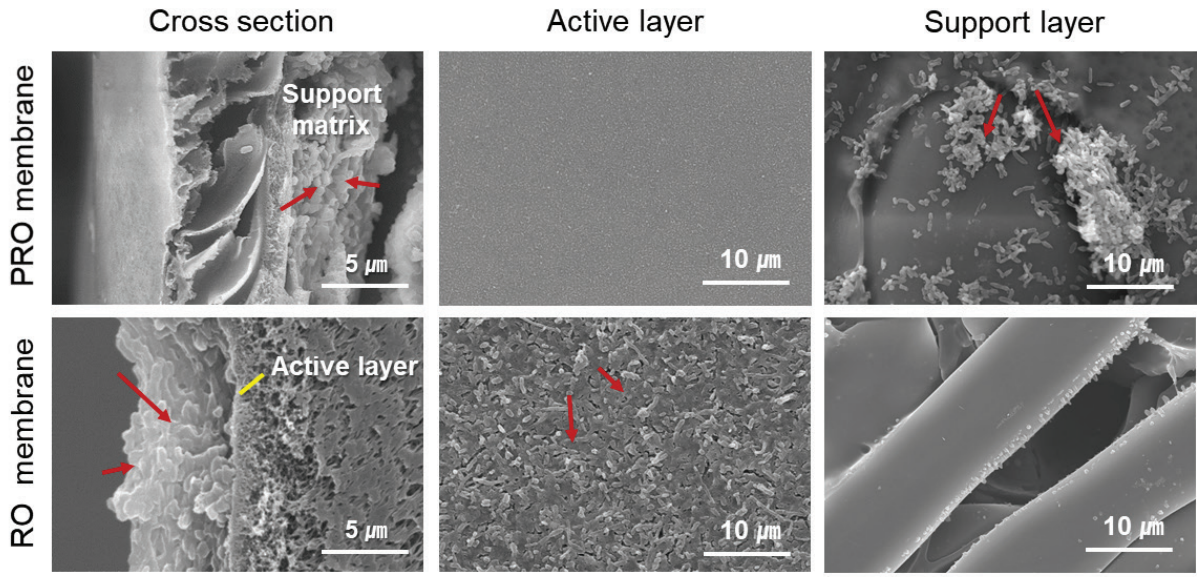

Fig. 8. SEM images of cross-section, active, and support layers of the PRO and RO membranes after cessation of the PRO unit (upper row) and the RO operation (lower row). Arrows indicate accumulation of bacterial cells.

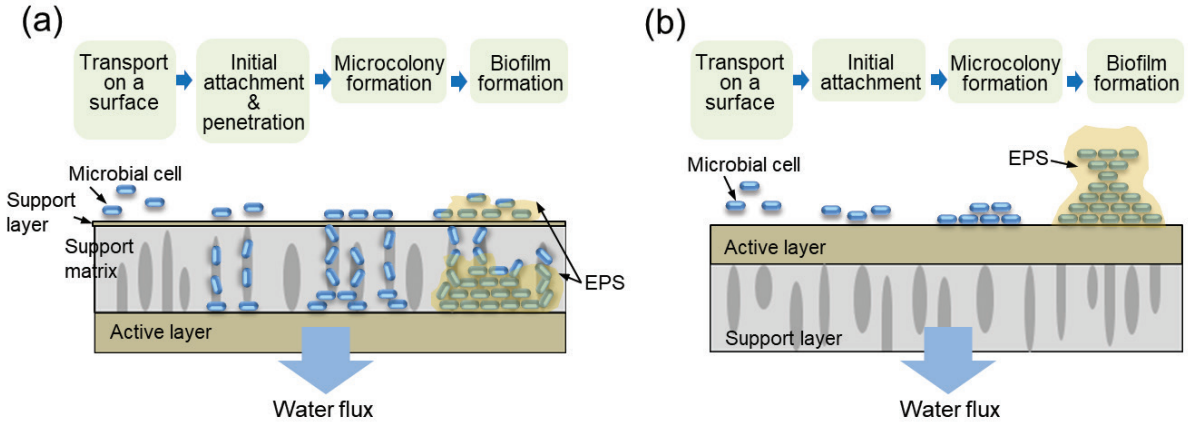

Fig. 9. A proposed conceptual model of the biofouling development on the PRO membrane (a) and the RO membrane (b).

the membrane surface (active layer in RO), attach onto the surface, and form biofilms in the RO membrane. However, microorganisms would not be able to pass through the dense active layer of the RO membrane, which would cause a delayed flux decline.

5. Conclusions

To obtain insight into biofouling in the PRO process, in this study, analysis was carried out on the physical and chemical properties of a model PRO membrane, biofilms were formed on the membrane, and a PRO unit was operated under an enhanced biofouling condition. The physical and chemical properties of the PRO membrane determined the degree of biofilm formation on the support layer by influencing the interactions between microorganisms and the surface. Additionally, microorganisms entered the support matrix of the PRO membrane and formed biofilms, mainly due to the operational feature (i.e., water permeation from support layer to active later) and structural property of the PRO membrane (loose support layer). This accelerated flux declines during the operation of the PRO unit, and will eventually affect power production. In order to retard the biofouling in the support matrix, the entrance of the microorganisms into the support matrix needs to be reduced, possibly through extensive pretreatment and/or substitution of a membrane with a support layer that can protect a passage of microorganisms.

Acknowledgments

This research was supported by funds from the Ministry of Land, Infrastructure and Transport (MLIT;

16IFIP-B065893-04) and the National Research Foundation (NRF) of Korea (2016R1A6A3A11935079), and a grant from the Korea University.

References

[1] S. Loeb, Osmotic power plants, Science, 189 (1975) 654–655.
[2] B.E. Logan, M. Elimelech, Membrane-based processes for sustainable power generation using water, Nature, 488 (2012) 313–319.
[3] S. Loeb, Production of energy from concentrated brines by pressure-retarded osmosis: I. Preliminary technical and economic correlations, J. Membr. Sci., 1 (1976) 49–63.
[4] S. Loeb, Large-scale power production by pressure-retarded osmosis, using river water and sea water passing through spiral modules, Desalination, 143 (2002) 115–122.
[5] G.Z. Ramon, B.J. Feinberg, E.M. Hoek, Membrane-based production of salinity-gradient power, Energy Environ. Sci., 4 (2011) 4423–4434.
[6] E. Bar-Zeev, F. Perreault, A.P. Straub, M. Elimelech, Impaired performance of pressure-retarded osmosis due to irreversible biofouling, Environ. Sci. Technol., 49 (2015) 13050–13058.
[7] D.I. Kim, J. Kim, H.K. Shon, S. Hong, Pressure retarded osmosis (PRO) for integrating seawater desalination and wastewater reclamation: energy consumption and fouling, J. Membr. Sci., 483 (2015) 34–41.
[8] N.Y. Yip, M. Elimelech, Influence of natural organic matter fouling and osmotic backwash on pressure retarded osmosis energy production from natural salinity gradients, Environ. Sci. Technol., 47 (2013) 12607–12616.
[9] W. Guo, H.-H. Ngo, J. Li, A mini-review on membrane fouling, Bioresour. Technol., 122 (2012) 27–34.
[10] H.-C. Flemming, Reverse osmosis membrane biofouling, Exp. Therm. Fluid Sci., 14 (1997) 382–391.
[11] H.-C. Flemming, G. Schaule, T. Griebe, J. Schmitt, A. Tamachkiarowa, Biofouling—the Achilles heel of membrane processes, Desalination, 113 (1997) 215–225.
[12] N. Prihasto, Q.-F. Liu, S.-H. Kim, Pre-treatment strategies for seawater desalination by reverse osmosis system, Desalination, 249 (2009) 308–316.
[13] A. Sagiv, R. Semiat, Backwash of RO spiral wound membranes, Desalination, 179 (2005) 1–9.
[14] S. Siavash Madaeni, T. Mohamamdi, M. Kazemi Moghadam, Chemical cleaning of reverse osmosis membranes, Desalination, 134 (2001) 77–82.
[15] S.S. Madaeni, S. Samieirad, Chemical cleaning of reverse osmosis membrane fouled by wastewater, Desalination, 257 (2010) 80–86.
[16] W.S. Ang, S. Lee, M. Elimelech, Chemical and physical aspects of cleaning of organic-fouled reverse osmosis membranes, J. Membr. Sci., 272 (2006) 198–210.
[17] A.P. Straub, A. Deshmukh, M. Elimelech, Pressure-retarded osmosis for power generation from salinity gradients: is it viable? Energy Environ. Sci., 9 (2016) 31–48.
[18] M. Herzberg, M. Elimelech, Biofouling of Reverse Osmosis Membranes: Role of Biofilm Enhanced Osmotic Pressure, H.C. Flemming, G.G. Geesey, Eds., Biofouling and Biocorrosion in Industrial Water Systems, Springer Publishing, Berlin, Germany, 1991, pp. 81–111.
[19] A. Matin, Z. Khan, S.M.J. Zaidi, M.C. Boyce, Biofouling in reverse osmosis membranes for seawater desalination: phenomena and prevention, Desalination, 281 (2011) 1–16.
[20] S. Tsuneda, H. Aikawa, H. Hayashi, A. Yuasa, A. Hirata, Extracellular polymeric substances responsible for bacterial adhesion onto solid surface, FEMS Microbiol. Lett., 223 (2003) 287–292.
[21] H. Ridgway, J. Safarik, Biofouling of Reverse Osmosis Membranes, Biofouling and Biocorrosion in Industrial Water Systems, Springer, 1991, pp. 81–111.
[22] T.-S. Kim, H.-D. Park, Lauroyl arginate ethyl: an effective antibiofouling agent applicable for reverse osmosis processes producing potable water, J. Membr. Sci., 507 (2016) 24–33.
[23] J.R. Goff, P. Luner, Measurement of colloid mobility by laser Doppler electrophoresis: the effect of salt concentration on particle mobility, J. Colloid Interface Sci., 99 (1984) 468–483.
[24] T.-S. Kim, H.-D. Park, Tributyl tetradecyl phosphonium chloride for biofouling control in reverse osmosis processes, Desalination, 372 (2015) 39–46.
[25] J.W. Costerton, P.S. Stewart, E.P. Greenberg, Bacterial biofilms: a common cause of persistent infections, Science, 284 (1999) 1318–1322.
[26] A. Subramani, E.M.V. Hoek, Direct observation of initial microbial deposition onto reverse osmosis and nanofiltration membranes, J. Membr. Sci., 319 (2008) 111–125.
[27] J. Yang, R. Bos, G.F. Belder, J. Engel, H.J. Busscher, Deposition of oral bacteria and polystyrene particles to quartz and dental enamel in a parallel plate and stagnation point flow chamber, J. Colloid Interface Sci., 220 (1999) 410–418.
[28] K. Marshall, R. Stout, R. Mitchell, Mechanism of the initial events in the sorption of marine bacteria to surfaces, Microbiology, 68 (1971) 337–348.
[29] J. Palmer, S. Flint, J. Brooks, Bacterial cell attachment, the beginning of a biofilm, J. Ind. Microbiol. Biotechnol., 34 (2007) 577–588.
[30] A.A. Myint, W. Lee, S. Mun, C.H. Ahn, S. Lee, J. Yoon, Influence of membrane surface properties on the behavior of initial bacterial adhesion and biofilm development onto nanofiltration membranes, Biofouling, 26 (2010) 313–321.
[31] B. Tansel, J. Sager, J. Garland, S. Xu, L. Levine, P. Bisbee, Biofouling affinity of membrane surfaces under quiescent conditions, Desalination, 227 (2008) 264–273.
[32] W. Lee, C.H. Ahn, S. Hong, S. Kim, S. Lee, Y. Baek, J. Yoon, Evaluation of surface properties of reverse osmosis membranes on the initial biofouling stages under no filtration condition, J. Membr. Sci., 351 (2010) 112–122.
[33] M. Van Loosdrecht, J. Lyklema, W. Norde, G. Schraa, A. Zehnder, The role of bacterial cell wall hydrophobicity in adhesion, Appl. Environ. Microbiol., 53 (1987) 1893–1897.
[34] S. Parkar, S. Flint, J. Palmer, J. Brooks, Factors influencing attachment of thermophilic bacilli to stainless steel, J. Appl. Microbiol., 90 (2001) 901–908.
[35] P. Parment, C. Svanborg-Ede'n, M. Chaknis, A. Sawant, L. Hagberg, L. Wilson, D. Ahearn, Hemagglutination (fimbriae) and hydrophobicity in adherence of *Serratia marcescens* to urinary tract epithelium and contact lenses, Curr. Microbiol., 25 (1992) 113–118.